DETECTION OF THE DEFECT OF SOLAR CELLS USING BASED ON UAV INFRARED REMOTE SENSING

Peng Zhang, Lifu Zhang*, Yi Cen, Hongming Zhang, Qingxi Tong

Institute of Remote Sensing and Digital Earth, Chinese Academy of Sciences Beijing 100101, China.

ABSTRACT: Research group set an infrared remote sensing system based on UAV, and utilized the system to detect defect of solar cells at Haier Company in Foshan, Guangdong province. It proven the feasibility of utilizing the system to detect the abnormal of solar cells. After acquiring images, the K-nearest neighbor filter was used in preprocessing, and identify and extract the single solar photovoltaic module from every image. And using with local and global anomaly detection method proposed by research group successfully extracts the anomalous area. The study results show that the infrared remote sensing base on UVA platform to detect the defect of solar cells gives full play the UVA's flexibility, and have strong detection capacity to the defect of a large area of solar cells at outdoor, and has the potential to be used in practice.

1. INTRODUCTION

Solar energy as a clean, environmental, sustainable, and renewable energy, has become a response to the energy shortage, climate change and energy saving and emission reduction. And the prospects for large-scale use also favored by countries (Sekone,2016). Martin Green who is known as the "father" of the solar energy and the Nobel Prize winner of the environment, pointed out that the proportion of photovoltaic solar in the whole world energy structure only accounted for about 0.02%. However, over the next 20 years, it is likely to be promoted to 25%. Dr. Alan Titchmarsh' research in energy alternatives of the world trend show that solar energy in the 21st century has entered a rapid development stage, and around 2050 reached 30%,which is second to nuclear power. It will replace nuclear energy as the first in the late 21st century. As a result, the great development and utilization of solar energy will be the mainstream of future energy use (Vanek, 2010).

In the use of several years late, due to the external force factors such as weathering, solar cells can cause surface pollution and damage. It can directly lead to adverse consequences such as reduction of the power generation efficiency. Detection of the defect of solar cells methods mainly include artificial detection, the laser detection (Tseng, 2015), electroluminescence detection (Tsai, 2015) and infrared imaging detection. Artificial detection is often inefficient and liable to mistakes. The laser detection and electroluminescence detection are not suitable for outdoor large-scale detection (Jiang, 2011).International and domestic academics with thermal infrared imaging method for the study of solar cells detection, mainly include: Ya-li Wang (Wang, 2015) put forward through the temperature difference at the surface of solar cells determine solar surface is stained. Pei-zhen Wang （ Wang，

2010）presents a state analysis and automatic identification method for solar cells based on infrared image.

On the basis of the above research, for the large-scale outdoor stained solar cells. This paper proposes a fast detection method based on UVA infrared remote sensing. The method utilize the system to collect image data. And through the data processing and analysis, we finally able to quickly determine the accurate position of the defect of solar cells.

2. EXPERIMENTATION

2.1 UAV Infrared Remote Sensing

2.1.1 UAV platform

The way of unmanned aerial vehicle (uav) low attitude flight is one of important spatial data acquisition methods. The method is of low cost and can obtain relatively high resolution images.UAV platform is mainly divided into fixed wing UAV and rotor UAV. Fixed wing flies relatively stable, but requires a runway or aircraft catapult.And rotor UAV for take-off venue request is not high. Taking account of such solar cells are laid in the factory building roof or nearby. The rotor UAV should be selected in preference. In addition to considering the lightweight load,small flight area and rotor UAV relatively poor stability problem, electric rotor UAV further is selected as a flying platform.The platform not only has the above advantages, but also the operation is relatively simple, and the vibration is small.

To sum up, in experiments, Spreading Wings S1000 (DJI inc.) is selected as the platform, which is an electric rotor UAV, and shows in fig.1. It is designed to carry payloads weighing up to 6.8kg. The technical data sheet show in table 1.

Fig.1 The real product of DJ-S1000

Table 1 DJ-S1000 technical data sheet

DJ-S1000	
type	Eight rotor aircraft
Takeoff Weight	6.0kg~11.0kg
Total Weight	4.2Kg
Power Battery	LiPo (6S, 10000mAh~20000mAh, 15C(Min))
Max Power Consumption	4000W
Hovering Power Consumption	1500W (@9.5Kg Takeoff Weight)
Hovering Time	15min (@15000mAh& 9.5Kg Takeoff Weight)
Working Environment Temperature	-10℃ ~ +40℃

2.1.2 thermal infrared payload

In this system, the modified Tau2 LWIR Thermal Imaging Camera Cores (FLIR Inc.) is utilized. The type of the camera is Uncooled VOx Microbolometer, and the specific parameters are given in table 2. The spectral response of the camera covers in the range of 7.5 to 13.5 μm, which meet the application requirements. In order, to meet the UAV platform demands, a 19mm lens was mounted on the camera, and our team specifically developed a data storage module for it. By using the storage module the acquired image and GPS data directly store to a removable storage medium with USB interface. After the mission ends, the date could be imported to the processing computer to process from the removable storage medium. A dual trigger device was developed for it, one is used to trigger the camera shutter, and the other mark the GPS date, which makes the image data and GPS data can be one to one correspondence, 5v Lithium batteries are used to provide power for it. The real product of IR loading is shown at fig. 2.
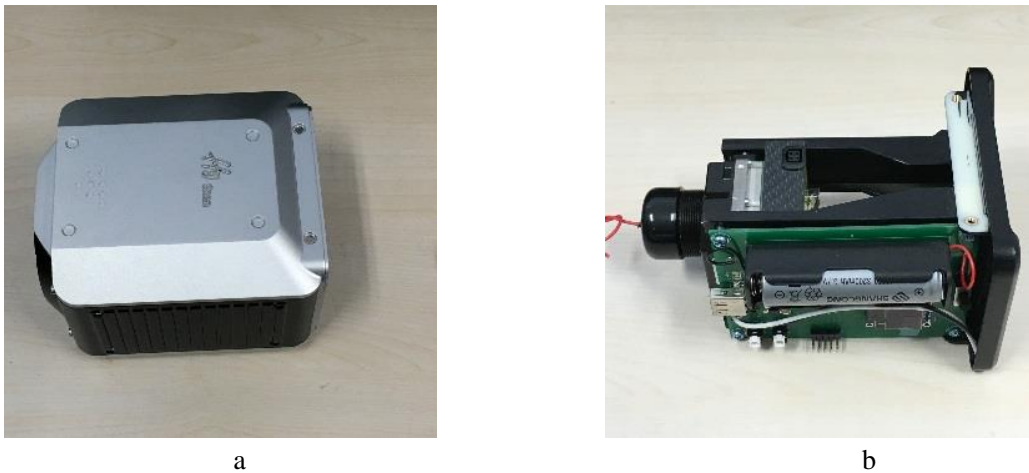

a   b

Fig.2 the real product of IR loading （a:the appearance b:the internal structure）

Table 2 Tau 2 technical data sheet

Tau2	
Thermal Imager type	Uncooled VOx Microbolometer
FPA/Digital Video Display Formats	640*512
Pixel Pitch	17μm
Spectral Band	7.5-13.5μm
Exportable Frame Rates	<9Hz
Sensitivity (NEdT)	<50 mK at f/1.0
Format	JPEG (8 bit) / TIFF (14 bit)或 mp4
Digital Zoom	2x, 4x, 8x
working voltage	4-6vDC
Working Environment Temperature	-40-80℃
Dimensions	60x54x15mm
Weight	45g

2.2 Data Acquisition

A factory is chose as the experimental area, which is located in Foshan, Guangdong province, China (23.25 N, 112.98 E). Large area of solar cells neatly laid out workshop roof, which provides power to this factory. The solar cells on the NO.3 workshop roofs were selected as the experimental sample. The sample region is shown at fig.3. Data were collected on at October 26, 2015, 10:00 to 12:00 am local time, under calm winds, cloudless conditions. The experiment completed two flight at speed of 2m/s, at relative altitude of 20m,40m(relative to the solar cells), and the ground resolution less than 0.03m. This experiment collected 1078 images date and corresponding GPS date.

Fig.3 Sample region

3. DATA PROCESSING

After sorting out the date, 712 image data is preserved (filtering the invalid image at the uninteresting region). The raw image data was stored as.PNG format, and the size of the image data is 1.02MB, and the image pixel is 701*512. Fig.4 is the flowchart of date processing.
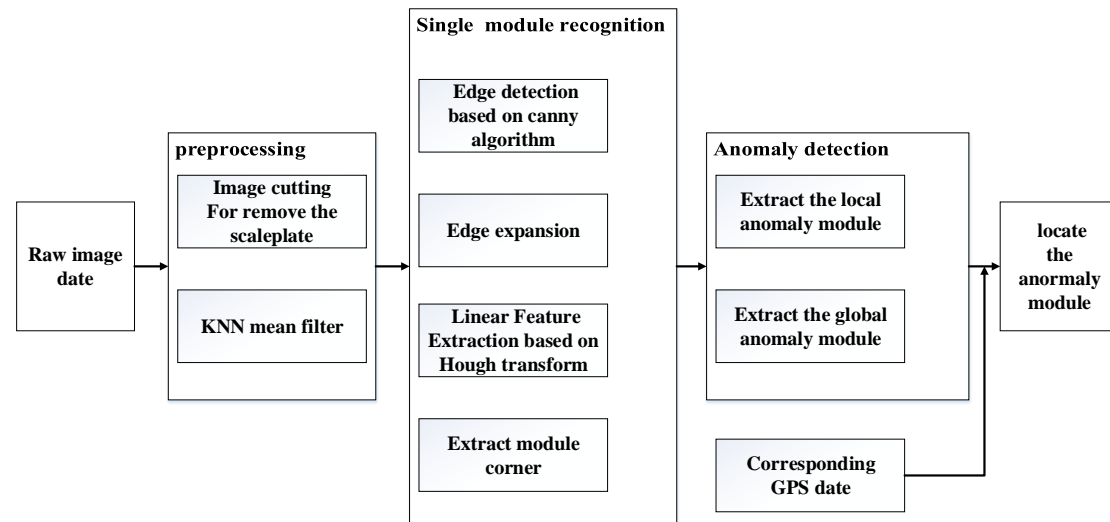

Fig. 4 Flowchart of data processing

3.1 Preprocessing

On the right side of the raw image data has a grayscale scaleplate, which increases difficulties in data processing. Given that the size and location of the scaleplate are fixed, all raw data can be cut into 640*512.

Due to the impact of the thermal infrared camera itself and the outside factors, the image data appear some problems, such as fuzzy boundary, salt-and-pepper noise, on-uniformity etc. In the paper we adopt the median filtering, the Gaussian low-pass filter and the K-nearest neighbor filter. The three filtering methods are all have a certain effect to eliminate the noise.However, the median filtering and the Gaussian low-pass filter fuzzy up the linear feature. So this article uses k-nearest neighbor filter to preprocess the raw date.

3.2 Single Photovoltaic Module Recognition

The key to anomaly extracting is to definite the anomaly characteristics. In this paper, raw image data was acquired based on the UAV platform. However, the stability of the platform is lower than the laboratory or the ground image acquisition platform. Besides, the uniformity of single-channel IR image is poor. A limited number of reliable features can be used in these grayscale images. Hence, to locate the solar panel defects are difficult on the full solar photovoltaic panels. Considering the single photovoltaic module arranges neatly on the solar panels, and the DN value of the edge is lower, which form grid pattern. To extract every single photovoltaic module for analysis greatly reduces the difficulty of anomaly detection.

According to the single photovoltaic module above characteristics, the edge of the single photovoltaic module should be extracted in the first step. Edge refers to the boundary of the image object, namely the curves of DN value of drastic changes in the image. Through researched on the current main edge

algorithm, such as canny, sobel, prewitt, Roberts, etc., to compare other algorithm, the canny algorithm use two gradient threshold, which has strong denoising ability and higher precision . So, canny algorithm was adopted to detect the edge in the paper. After edge detection, there are incontinuous edges in some modules, which directly affect the linear feature extraction. So the algorithm of expansion is used to deal with the incontinuous problem. In this paper, the Hough Transform was used for linear feature extraction. According to the principle of Hough Transform. The linear feature extraction equates to line detection, and the essence of it is to find all the pixels which form the line. The key is to find all the point (x,y) which is match with y=mx+c. the coordinate system is witch from y=mx+c to c=-mx+b. After that, each point(x1,y1) on this line becomes to a line, and those lines cross at a point (m,c) in MC coordinate system. The problem of finding all the point changes the problem of finding a line. Each point in the image corresponds to many lines in MC coordinates. If the intersection of these lines is found, we also find the line in the image. Using $Y = KX + C$ on implementation, there will be a lot of limitations, the formula 1 will break this limitation.

$$Rho = xcos（theta）＋ysin（theta）\qquad\qquad (1)$$

Rho is the distance from point to line, theta is angle between the line with x-axis.

Linear feature concentrate on the edge of the module, linear features are divided into two types, horizontal and vertical line, respectively. The slope of each type is similar. If all the slope were calculated, the horizontal or vertical edge line will be found. In order, to get the position of each module, the intersections of the two type lines were calculated. Then four adjacent intersections are from a module. Some micro-regions which are not the module were extracted falsely. Because the length-width ratio of the module is relatively fixed, approximately 2:1. Dismiss the regions that do not meet the principle. The nomenclature of each module is the image number plus the column number of the recognized module. For example module numbers for 1-017-1-1, the meaning is that the module locates the first line and first column in image which is the 17th image in the first flight.

3.3 Anormaly Detection

Because part or all of module is the dirty, it leads to photoelectric conversion works abnormally. The temperature of this module surface is higher than others. So the abnormity is defined temperature of the region is higher than the mean temperature of the region. The abnormity can be divided into two kinds: one is the local abnormity, namely there are ligthspots or cracks on the module; and the other is the global abnormity, which needs to be detected in module level instead of each module. Combined with the results of local and global anomaly analysis,will get the final detection results.

Considering the image is relatively simple, and there are numerous images data, and the requirement of rapid processing, threshold dichotomy to be used for detection. Calculation formula of threshold value as showed in equation 2.

$$Thresh = med + std \qquad\qquad (2)$$

When the local anomaly is detected, the med is the average value of each module pixel DN, and std is standard deviation of each module pixel DN. If the pixel DN. Is larger than the threshold, the pixel is determined as an abnormal pixel. If the number of the abnormal pixel more than one percent of the total number of the module pixel. The module is defined as an abnormal module and then serial number of the module should be returned.

When the global anomaly is detected, the med is the average value of all module pixel DN, and std is standard deviation of all module pixel DN. If the average value of a module pixel DN is larger than the threshold. The module is defined as an abnormal module and then serial number of the module should be returned.

According to the serial number of the module and the corresponding GPS data, the abnormal module can be precisely located

4. EXPERIMENTAL RESULTS

According to the article 2.1 and 2.2, the image data is processed. With the image 1-017, the preprocessing and the results of single module recognition are shown.Raw thermal infrared image after cutting is shown in figure 5 (a).For K neighbor average filtering images, the result is shown in figure 5 (b). the results of edge detection based on canny operator are shown in figure 6 (a); Then the line which is detected expanse based on expansion algorithm,and   the result is shown in figure 6 (b);As shown in figure 6 (c), the figure is the results of   linear feature extraction based on hough transform. As showed in figure 6 (d), which is the selected module edge straight; as showed in Figure 6 (e), which is the corner of the module; the extracted module results are shown in table 3.
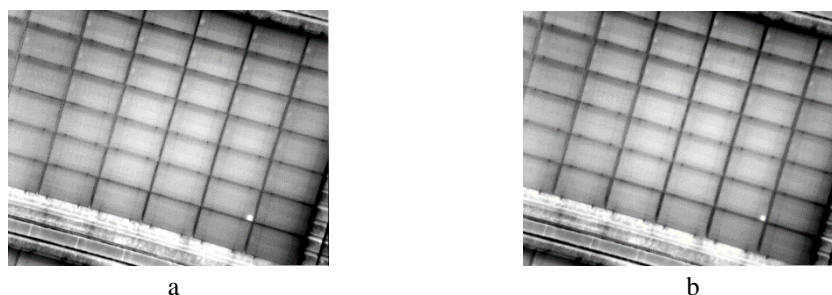

a   b
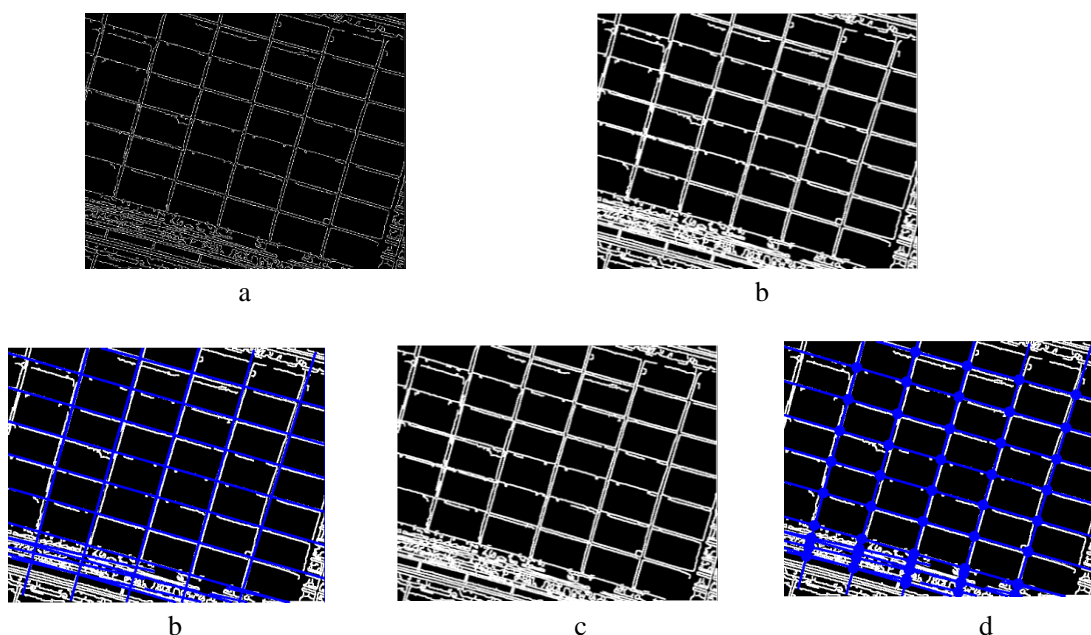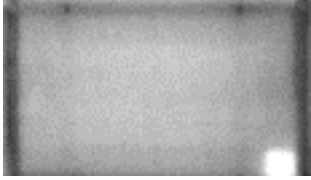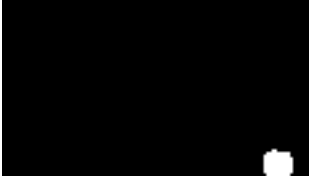
Fig. 5 filtering result（a:the raw image,b:the result image）

a   b

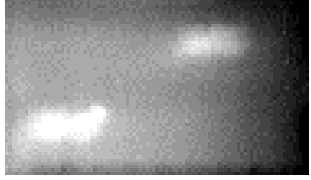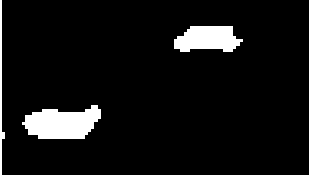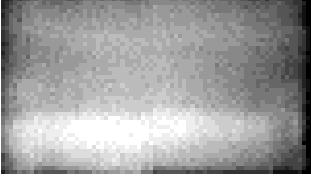b   c   d

Fig. 6 Results of different steps in the model recognition （a: the result of edge detection,b:the result of expansion arithmetic,c:the result of line detection,d:the result of filtered the edge of module,e:the result of the intersections of module）

Table 3 Module extraction results

	1	2	3	4
1				
2				
3				
4				
5				
6				

According to the article 2.3, anomaly detection method is used into each image based on global of local anomaly detection and anomaly detection. As showed in table 4, this is a local anomaly detected abnormal module: 1-017-5-4, 1-287-3-5 and 488-6-4.As showed in figure 7, it is to use global anomaly detection method to detect abnormal module: 646-3-1 and 646-4-1.

Table 4 The result of local anomaly detection

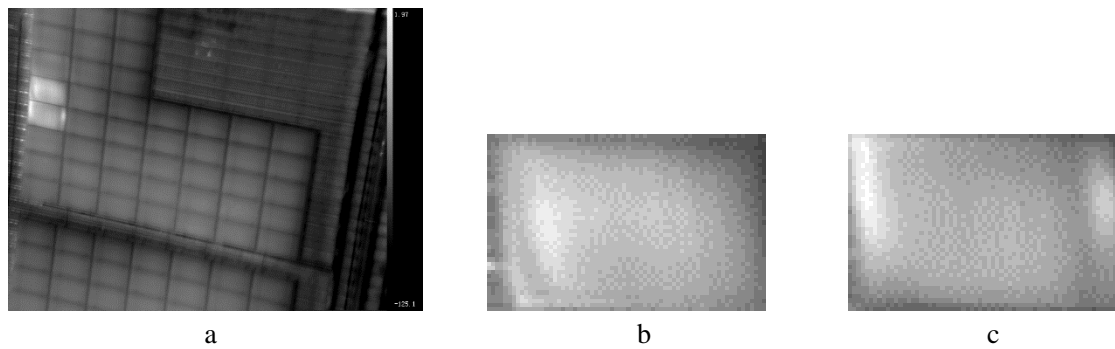| 编号	原影像	提取结果
1-017-5-4		
1-287-3-5		
1-488-6-4		

a   b   c

Fig. 7 the result of global anomaly detection (a: The raw image, b,c: The result of global anomaly detection)

5. CONCLUSION

In this work, we propose a solar panels defect rapid detection and location based on UVA infrared remote sensing method. When tested using real world from a plant, the method demonstrated good performance, including effective and quick detection and precise location. At the same time, it also proves that the infrared remote sensing system based on UAV platform has a good detection capability for solar panel defect, and also has a high value of practical application.

References

Sekone a k, Chen yu-bin, Lu ming-chang, et al. 2016. Silicon Nanowires for Solar Thermal Energy Harvesting: an Experimental Evaluation on the Trade-off Effects of the Spectral Optical Properties .Nanoscale Research Letters, 11(1), pp: 1

Vanek J, Stencel J. 2010. System for an automatic analysis of defective Solar cells in the Solar Module. ActaMontanistica Slovaca, 15, pp: 105-110

Tseng D C, Liu Yu-Shuo, Chou Chang-Min. 2015. Automatic Finger Interruption Detection in Electroluminescence Images of Multicrystalline Solar Cells. Mathematical Problems in Engineering, pp: 12

Tsai D M, Li Guan-Nan b, Li Wei-Chen a, et al. 2015,.Defect detection in multi-crystal solar cells using clustering with uniformity measures . Advanced Engineering Informatics, 21(9), pp: 419-430

Jiang Xiao-Yu, Wang Chao, Wang Xi, et al. 2011. Defects detection in crystalline silicon solar cells based on electroluminescence imaging , Proceedings of SPIE

Wang Ya-li. 2015. Research and method of defect detection of solar panels based on infrared imaging. measurement&control technology. 34(7) , pp:59

Wang Pei-zhen. 2010. Fault analysis of photovoltaic array based on infrared image. Journal of solar energy. 34(7), pp: 59